# Phonons in {110} surfaces of III-V compound semiconductors

Hermann Nienhaus*
*Laboratorium für Festkörperphysik, Gerhard-Mercator-Universität Duisburg, D-47048 Duisburg, Germany*
(Received 31 March 1997)

High-resolution electron energy-loss spectroscopy was applied to determine phonon dispersions of cleaved AlSb(110), GaP(110), GaSb(110), and InAs(110) surfaces. Besides the acoustic surface waves and the optical Fuchs-Kliewer modes additional flat phonon bands were detected in all materials. The experimental results agree very well with recent *ab initio* calculations of surface phonon dispersion curves. For GaP(110), several phonon modes are observed within the fundamental gap between acoustic and optical bulk phonon bands. In AlSb(110) a gap mode is detected very close to the bulk optical band edge whereas the GaSb gap is free of surface-localized states. The measurements confirm theoretical predictions that significant gap modes exist at these surfaces if the anion mass is smaller than the cation mass. For the acoustic and the Fuchs-Kliewer modes chemical trends are demonstrated. The differences of the excitation energies in the materials considered depend only on the anion and cation masses as well as the nearest-neighbor distances. [S0163-1829(97)08643-8]

## I. INTRODUCTION

Experimental and theoretical investigations of surface phonon dispersions have witnessed rapid progress during the last decade. Profound studies on surface dynamics have become possible by the development of high-resolution energy-loss spectrometers for electron and He atom scattering and of first-principles calculations.[1–3] To measure dispersion curves along the main symmetry directions of the surface Brillouin zone (s-BZ) the background signal, by virtue of diffuse scattering, must be effectively reduced. Hence, well-ordered and flat surfaces of excellent quality are required. There are only a few experimental investigations for III-V compound semiconductors. Studies on cleaved GaAs(110), InP(110), and InSb(110) surfaces[4–8] have been reported so far.

In particular, GaAs was the first III-V compound semiconductor for which surface phonon dispersions were measured by use of He atom scattering (HAS) (Refs. 4 and 5) and high-resolution electron energy-loss spectroscopy (HREELS).[6] A variety of theoretical models have been applied to the GaAs(110) surface as well. They were based on nearest-neighbor force constants,[9] tight-binding methods,[10–13] bond charge concepts,[14–17] and, recently, *ab initio* theories.[18–21] Especially the results using the density-functional perturbative scheme by Fritsch, Pavone, and Schröder[18] described the experimental data very well. Shortly after that, a HREELS study of InP(110) phonons[7] revealed surface-localized modes within the gap between optical and acoustic bulk phonon bands. Such gap modes were predicted by Das and Allen in a simple theoretical approach.[9] Subsequent *ab initio* and bond charge calculations[22,23] agreed excellently with the experimental results. They clarified the character of InP(110) gap modes. The calculated displacement patterns indicate that the top P atoms are moving with large amplitudes whereas the ln atoms are almost at rest.[22]

These findings motivated further calculations on the lattice dynamics of other III-V(110) surfaces, in particular, AlAs, GaSb, GaP, and InAs.[17,20,24] It was concluded that gap modes as observed in InP(110) exist if the surfaces exhibit a relaxation and if the anion mass is smaller than the cation mass. In the opposite case of larger anion masses, the gap is expected to be free of surface states, as predicted for GaSb(110), or gap modes may appear very close to the optical bulk band edge.

The present HREELS study will show phonon dispersion data for (110) surfaces of AlSb, GaSb, GaP, and InAs single crystals. These materials exhibit fundamental gaps between acoustic and optical bulk phonons. Thus, they are candidates to investigate the existence of gap modes and to check the theoretical predictions. Furthermore, chemical and mass trends for the surface optical Fuchs-Kliewer (FK) phonons[25] at the s-BZ center $\Gamma$ and for the surface acoustic waves will be deduced from the data. They have been proposed earlier from theoretical as well as experimental considerations.[2,17,20]

## II. EXPERIMENT

The experiments were performed at a base pressure of lower than $10^{-8}$ Pa. (110)-oriented surfaces of III-V compound semiconductors were prepared by cleaving bars of single crystals in a double-wedge technique. As pointed out elsewhere, broadening of the loss peaks in the HREEL spectra is effectively avoided by using semi-insulating material.[2,6,7] For the semiconductors considered in the present study, semi-insulating crystals were not available. The GaP and InAs samples were doped *n* type with a free-electron density of $6\times10^{17}$ cm$^{-3}$ and $5\times10^{16}$ cm$^{-3}$, respectively. The *p*-type GaSb crystals exhibited free carrier concentrations of $5\times10^{17}$ cm$^{-3}$. AlSb crystals are not commercially available. They were kindly provided by the Max-Planck-Institut of Solid State Research in Stuttgart. This material was nominally undoped. However, the linewidths in the HREEL spectra exceed the instrumental resolution by far. This indicates a density of free charge carriers much higher than known from semi-insulating semiconductors. It may be due to bulk defect states in AlSb. Furthermore, AlSb(110) surfaces exhibit a high affinity to oxygen in contrast to other III-V(110) surfaces. After cleavage, measurements had to be accomplished within a few hours even under the best ultrahigh vacuum conditions.

 

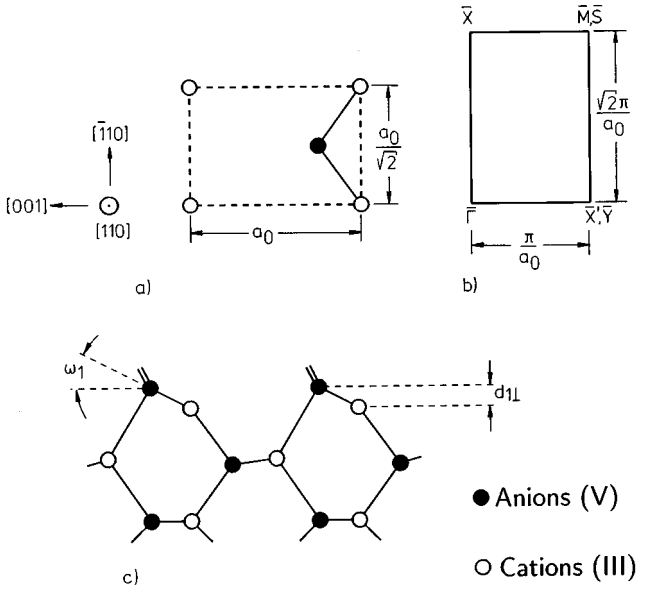


FIG. 1. Structure of relaxed III-V(110) surfaces: (a) surface unit mesh; $a_0$ is the lattice constant; (b) quarter of the s-BZ; (c) side view along the cation-anion chains in the [110] direction.

The experiments were carried out with a HREEL spectrometer comprising a double cylindrical deflector monochromator and analyzer.[26] The instrumental energy resolution was adjusted to typically 3 meV (24 $cm^{-1}$). The primary energy $E_p$ of the incident electrons varied between 5 and 100 eV. The angle of incidence $\vartheta_i$ ranged between 45° and 60° relative to the surface normal. The detection angle $\vartheta_s$ was kept constant at 60°. Hence, the absolute value of the parallel or surface wave vector transfer $\mathbf{q}_\parallel$ may be deduced from

$$q_\parallel = |\mathbf{k}_{i\parallel} - \mathbf{k}_{s\parallel}| = k_i \left| \sin\,\vartheta_i - \sqrt{1 - \frac{\hbar\omega}{E_p}}\,\sin\,\vartheta_s \right|, \qquad (1)$$

where $\mathbf{k}_{i\parallel}$ and $\mathbf{k}_{s\parallel}$ denote the parallel components of the wave vectors of the incoming and scattered electrons, respectively. The quantity $\hbar\omega$ represents the energy of the surface phonon or, generally, the surface excitation. The direction of the surface wave vector relative to the crystal orientation was determined by low-energy electron diffraction. In specular scattering geometry, when $\vartheta_i = \vartheta_s$, the parallel wave-vector transfer almost vanishes since the primary energy is by orders of magnitude larger than the phonon energies.

With electron scattering at ordered surfaces, energy and parallel wave vector are conserved.[27] Therefore, surface-phonon dispersions $\hbar\omega(\mathbf{q}_\parallel)$ may be measured by recording HREEL spectra in off-specular geometry.

## III. RESULTS

### A. Surface geometry

The rectangular two-dimensional unit cell of (110) surfaces of zinc-blende-structure III-V compound semiconductors is shown in Fig. 1(a). The surfaces exhibit a relaxation, i.e., the atoms in the top layers have different equilibrium positions compared to a truncated crystal.[28] Anion-cation zigzag chains in [110] direction are tilted by a bondlength-conserving rotation where the anions are pointing outwards. This is demonstrated in the cut view along the chains in Fig. 1(c). Consequently, the dangling bonds of anions and cations are doubly occupied and empty, respectively. The tilt angle $\omega_1$ and the normal displacement $d_{1\perp}$ of the topmost atoms depend on the lattice constant $a_0$ and the interatomic electrostatic energy. By use of low-energy electron diffraction $\omega_1$ and $d_{1\perp}$ were determined (references in Ref. 28). One obtained 27.5° and 63 pm for GaP(110), 30° and 77 pm for GaSb(110), 31° and 78–88 pm in the case of InAs(110). The relaxation parameters of AlSb(110) have not been measured, yet. However, they were recently calculated.[3] The authors reported values of 33.5° and 82.7 pm.

### B. HREEL spectra

A quarter of the respective s-BZ with the notations of the main symmetry points is given in Fig. 1(b). HREEL spectra were recorded from GaSb(110) and AlSb(110) with $\mathbf{q}_\parallel$ in the $\overline{\Gamma X}$ direction, i.e., along the zigzag chains. For GaP(110) and InAs(110), spectra were taken in $\overline{\Gamma X'}$ direction, i.e., perpendicular to the anion-cation chains. At all surfaces, many HREELS measurements were carried out at various primary energies. In the following a few spectra will be presented as examples.

At $\Gamma$, i.e., in specular scattering geometry, where $\vartheta_i \approx \vartheta_s$ and $\mathbf{q}_\parallel \approx \mathbf{0}$, inelastic electron surface scattering is governed by interaction via longrange electric dipole fields.[1,29] In this so-called dipole scattering regime, cross sections may be well predicted by the use of dielectric theory. The count rates are large and the most prominent loss structures are due to excitations of macroscopic FK surface phonons and—in the case of highly doped semiconductors—of surface plasmons of free charge carriers. This is demonstrated in the top spectra of Figs. 2–5. They display dipole spectra recorded from (110) surfaces of AlSb, GaP, GaSb, and InAs. Anti-Stokes and Stokes lines are observed on the energy-gain and -loss side, respectively. The primary energy $E_p$ varies between 5 and 100 eV. FK phonon energies are found at 41.5 meV for AlSb, 49.6 meV for GaP, 28.5 meV for GaSb and 29.5 meV for InAs. The GaP and InAs data agree well with values reported by others.[30–32] The excitation energy of FK phonons in GaSb deviates from a value presented in an early HREELS study.[33] The authors measured an energy of 35 meV. However, they already mentioned that their value was too large to be explained in the framework of dielectric theory. The discussion will show that the smaller value for the FK phonon energy in GaSb(110) fits the chemical trend much better.

Loss structures due to excitation of surface plasmons of free charge carriers are only resolved in the dipole spectra of GaSb and InAs. In the top spectrum of Fig. 4, the peak of elastically scattered electrons from GaSb(110) exhibits an asymmetric profile. Shoulders appear at 10.4 meV on the energy-loss and -gain side. In case of InAs(110), the plasmon losses at 11.0 meV are well detected as separate structures as shown in Fig. 5. With $E_p = 100$ eV, they are even stronger than the FK features.

Outside the s-BZ center $\overline{\Gamma}$, measurements were performed with $\vartheta_i \neq \vartheta_s$. In this impact scattering regime the interaction may be explained by multiple electron-atom scattering

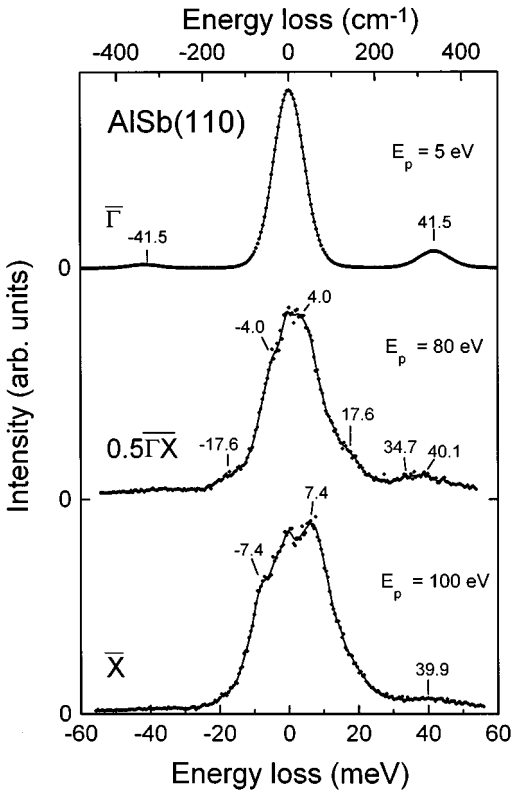


FIG. 2. HREEL spectra recorded from AlSb(110) at different points in the s-BZ along the $\overline{\Gamma X}$ direction; the top spectrum was measured in the dipole scattering regime.

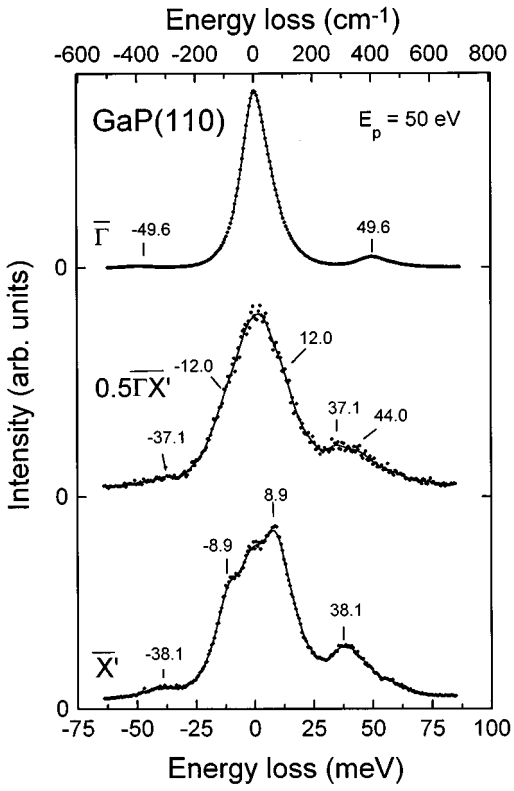


FIG. 3. HREEL spectra recorded from GaP(110) at different points in the s-BZ along the $\overline{\Gamma X'}$ direction; the top shows a dipole spectrum.

events in the surface layer.[1,29] The count rate is much lower and the dominant loss peaks are attributed to acoustic surface phonons. This is demonstrated in the middle and bottom spectra of Figs. 2–5. They show typical off-specular HREEL spectra at different points in the s-BZ. The solid lines through the data were calculated by a fast Fourier transform algorithm. The strongest loss lines are attributed to acoustic surface phonon modes $A$. For small surface wave vectors their excitation energies become larger with increasing $q_{\parallel}$. This is well observed in the spectra of AlSb(110), GaP(110), and GaSb(110) in Figs. 2–4. At the s-BZ boundaries $\overline{X}$ and $\overline{X'}$, respectively, one obtains acoustic phonon energies of 7.4 meV for AlSb, 8.9 meV for GaP, and 6.7 meV for GaSb. For InAs(110) surfaces, both impact spectra in Fig. 5 give acoustic phonon energies of 5.5 meV at the high-symmetry point $\overline{X'}$ as well as for a wave vector reaching into the second s-BZ.

Besides the acoustic modes, additional loss features are observed in the impact spectra of all four investigated semiconductors. For AlSb(110), Fig. 2 reveals structures at 17.6, 34.7, and 40.1 meV for $\mathbf{q}_{\parallel}=0.5\overline{\Gamma X}$. At the s-BZ boundary a weak loss is found at 39.9 meV. In the HREEL spectrum of GaP(110) in the middle of Fig. 3, shoulders around the peak of elastically scattered electrons are attributed to an energy loss at about 12 meV. Additionally, a double structure with peak energies of 37.1 and 44.0 meV is observed on the energy-loss side of the spectrum. With larger surface wave vector, i.e., at $\overline{X'}$, a broad peak at 38.1 meV is found. It does not exhibit a double structure any longer. With GaSb(110) and InAs(110) surfaces, electrons may excite an acoustic phonon and a surface plasmon of free charge carriers subsequently. This leads to combination loss structures in the HREEL spectra. A detailed analysis of the impact spectra from GaSb(110) shown in Fig. 4 reveals weak features at 14.9 meV for $\mathbf{q}_{\parallel}=0.4\overline{\Gamma X}$ and at 16.1 meV for the s-BZ boundary. They cannot be explained uniquely. They may be due to either combination losses or microscopic surface phonon modes. For InAs(110), subsequent excitations of $A$ phonons and plasmons are more clearly observed. The HREEL spectrum in the middle of Fig. 5 was recorded at $\overline{X'}$. It shows a structure comprising two peaks at about 17.3 and 21.7 meV. The low-energy component is definitely attributed to a combination excitation. The second one is due to a microscopic surface phonon. Likewise, the 20-meV loss at the bottom of Fig. 5 may be explained by a single excitation of a phonon mode. Here, the wave vector amounts to $1.4\overline{\Gamma X'}$ and, hence, reaches into the second s-BZ. This may be a way to detect phonons that are otherwise superimposed by combination losses.

### C. Dispersion diagrams

The four compound semiconductors considered in this study exhibit fundamental energy gaps between acoustic and optical bulk phonon bands. Therefore, one may find true surface-localized phonon modes that cannot couple resonantly to bulk states. Such surface phonons have excitation energies within this band gap. To examine the existence of gap modes $G$, dispersion diagrams are sketched in Figs. 6–9 for AlSb(110), GaP(110), GaSb(110), and InAs(110), re-

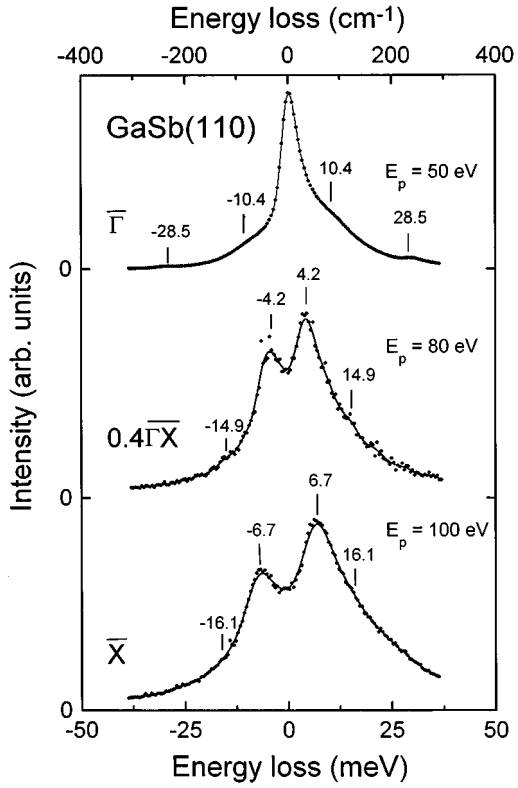


FIG. 4. HREEL spectra recorded from GaSb(110) at different points in the s-BZ along the $\overline{\Gamma X}$ direction; the elastic peak in the top dipole spectrum is asymmetrically broadened due to surface plasmons of free charge carriers.

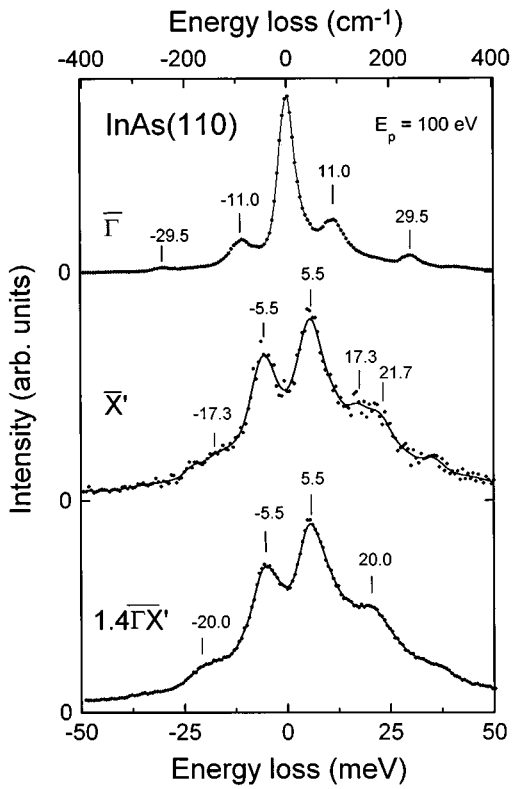


FIG. 5. HREEL spectra recorded from InAs(110) at different points in the first and second s-BZ along the $\overline{\Gamma X'}$ direction; the features at 11 meV in the dipole spectrum are due to surface plasmons of free charge carriers.

spectively. The surface phonon energies extracted from the HREEL spectra are plotted as a function of the surface wave vector $\mathbf{q}_{\parallel}$. The open circles are deduced from weak structures. Their loss energies were obtained after taking the first derivative of the data. The shaded areas and solid lines in Figs. 6–9 are calculated bulk phonon bands projected onto the s-BZ and theoretical dispersion curves, respectively. For AlSb(110), GaP(110), and InAs(110), the theoretical results were obtained from first-principles calculations using the density-functional approach.[3,24,34] For GaSb(110), a generalized mass approximation using force constants of GaAs(110) was applied.[3] This method gives reliable results as was verified at the main symmetry points in the s-BZ.

For AlSb(110) surfaces, the HREEL results in Fig. 6 give one acoustic branch *A* and four almost flat surface modes at about 8.5, 17.5, 35, and 40 meV. Due to a high diffuse scattering background no microscopic phonon modes were observed for wave vectors smaller than $2\times10^{9}$ m$^{-1}$. Two modes are found very close to the edges of the bulk phonon gap. To decide which one is a gap mode the experimental values of the longitudinal-acoustic (LA) and the transverse-optical (TO) phonon energies at the high-symmetry point *X* are included in Fig. 6. These frequencies are equivalent to the edges of the band gap. With inelastic neutron scattering at 15 K Strauch, Dorner, and Karch obtained 19.2 meV for the LA and 36.7 meV for the TO phonon.[35] The theoretical values of the band-gap edges are about 1 meV too small. Hence, only the mode found close to the AlSb optical band

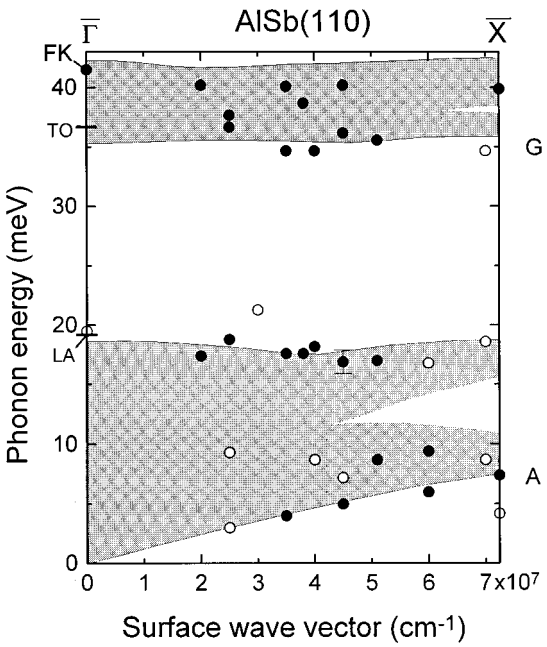


FIG. 6. Dispersion diagram for AlSb(110) surface phonons along $\overline{\Gamma X}$; shaded areas represent the projected bulk phonon bands taken from Ref. 34. The experimental TO and LA phonon energies are indicated on the left axis. Labels FK, *A*, and *G* give Fuchs-Kliewer, surface acoustic, and gap modes, respectively.

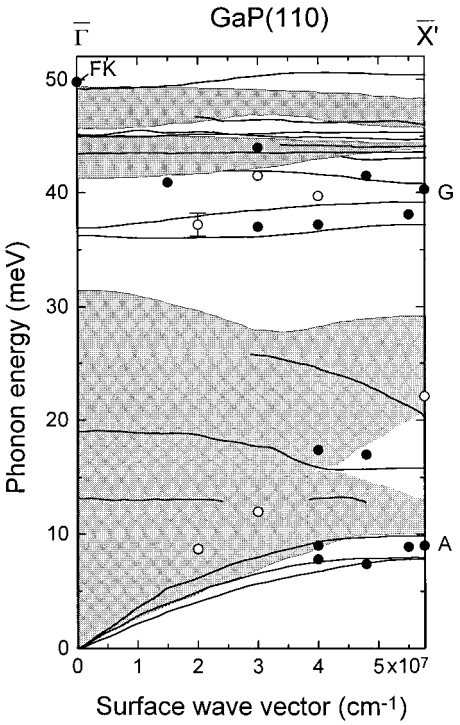


FIG. 7. Dispersion diagram for GaP(110) surface phonons along $\overline{\Gamma X'}$; shaded areas and solid lines represent calculated projected bulk phonon bands and surface phonon modes taken from Ref. 24. Labels FK, *A*, and *G* indicate Fuchs-Kliewer, surface acoustic, and gap modes, respectively.

minimum is identified as a gap phonon. Its energetic position is different compared to gap modes in InP(110) that are detected in midgap position.[7]

Theoretical and experimental results for GaP(110) surfaces shown in Fig. 7 agree quite well. The experiments give gap phonon modes in the energy range between 36 and 41.5 meV, i.e., in the upper half of the bulk phonon gap. The respective loss structures are broad and may be sometimes decomposed into several subpeaks. These findings indicate that more than one gap mode is excited by electron scattering, which is consistent with theory. It predicts three branches in this energy range. Also in the low-energy regime of the GaP(110) surface phonon spectrum, the measured data are close to calculated dispersion curves. Even the stomach-gap mode at about 17.5 meV is reproduced by two data points. This mode was not found in the studies of GaAs(110) and InP(110) surface phonons. Three acoustic bands along $\overline{\Gamma X'}$ resulted from theory. The intermediate mode is expected to have a shear-horizontal polarization as it was reported for InP and GaAs.[6,18,22] Hence, it cannot be excited by inelastic surface scattering. The upper and lower acoustic branches are not resolved with HREELS due to the large linewidths in the spectra.

The GaSb(110) dispersion diagram is displayed in Fig. 8. Remarkably, neither theory nor the experiments find surface-localized modes in the fundamental bulk phonon gap. Reasons for that will be discussed in the following chapter. As mentioned above, the loss structures between 15 and 20 meV cannot be interpreted uniquely since they may also be due to combination losses. For the acoustic modes, the experimental

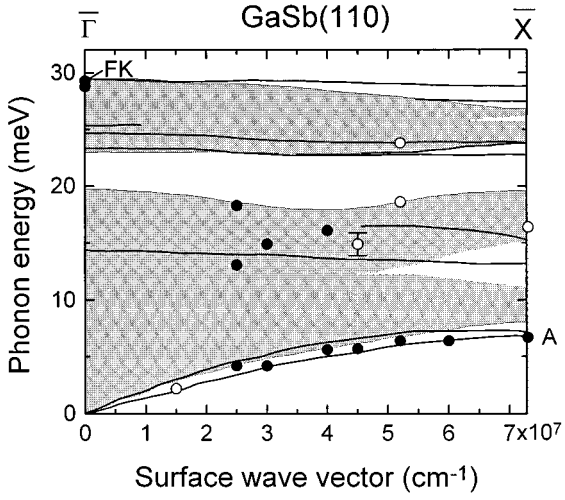


FIG. 8. Dispersion diagram for GaSb(110) surface phonons along $\overline{\Gamma X}$; shaded areas and solid lines represent calculated projected bulk phonon bands and surface phonon modes taken from Ref. 3. Labels FK and *A* indicate Fuchs-Kliewer and surface acoustic modes, respectively.

results are excellently described by theory. However, the two predicted branches cannot be separated in the measurements.

In the InAs(110) dispersion diagram shown in Fig. 9 energy losses in the gap region are only found outside the first s-BZ. Theory expects surface-localized vibrations in the band gap.[24] Inside the first s-BZ, the acoustic mode *A* and the FK phonon at $\overline{\Gamma}$ are detected. The squares in Fig. 9 represent loss peaks by virtue of a combination of surface plasmons and acoustic phonons or—at $\overline{\Gamma}$—of single plasmon excitation. As shown above, they dominate the HREEL spectra in this energy range so that microscopic surface phonons are not observed.

The essential values of the *A*, *G*, and FK surface phonon modes presented so far are listed in Table I. Experimental

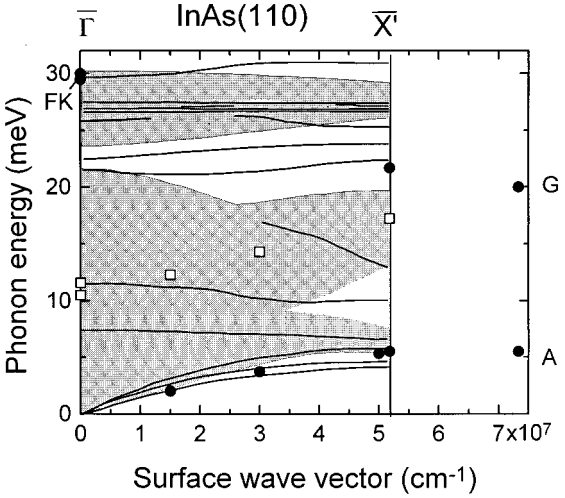


FIG. 9. Dispersion diagram for InAs(110) surface phonons along $\overline{\Gamma X'}$ in the first and second s-BZ; shaded areas and solid lines represent calculated projected bulk phonon bands and surface phonon modes taken from Ref. 24. Labels FK, *A*, and *G* indicate Fuchs-Kliewer, surface acoustic, and gap modes, respectively.

TABLE I. Excitation energies of acoustic surface ($A$), gap ($G$), and Fuchs-Kliewer (FK) phonons of III-V(110) surfaces. The values are given in meV.

| Mode | AlSb | GaAs (Refs. 4–6) | GaP | GaSb | InAs | InP (Ref. 7) | InSb (Refs. 8, 38) |
|---|---|---|---|---|---|---|---|
| $A$ at $\overline{X'}$ | | 6.2/7.0/7.5 | 8.9 | | 5.5 | 7.0 | 3.0/4.1 |
| $A$ at $\overline{X}$ | 7.4 | 8.5 | | 6.7 | | 8.4 | |
| $G$ in $\overline{\Gamma X'}$ | | no gap | 34–41.5 | | 20–21.7 | 30.5–33.5 | |
| $G$ in $\overline{\Gamma X}$ | 34.5–36.5 | no gap | | | | 30.5–33.5 | |
| FK at $\overline{\Gamma}$ | 41.5 | 35.8 | 49.6 | 28.5 | 29.5 | 42.3 | 24.0 |

data from the literature obtained with (110) surfaces of GaAs, InP, and InSb crystals are included. It should be remarked that from the available experimental and theoretical data the existence of a gap between acoustic and optical bulk phonons in InSb cannot be concluded.[36,37] If there is one it is certainly very small.

## IV. DISCUSSION

### A. Gap phonons

Gap modes at (110) surfaces of III-V semiconductors were found first at InP crystals.[7] They are located almost in the middle of the fundamental bulk phonon gap. Soon after the experimental evidence, *ab initio* calculations revealed the character of these vibrations.[3,22] Only atoms of the topmost surface layers are in motion. The displacement patterns show that the top $P$ atoms vibrate with large amplitudes. This result is due to the relaxation and the large mass difference between anions and cations. A similar situation is found with GaP and InAs. Likewise, theory predicts surface-localized modes with energies almost in the middle of the respective gaps.[3,24] The presented experimental data revealed such gap modes in GaP(110). In InAs(110), however, only at $\overline{X'}$ and in the second s-BZ, phonons are observed slightly above the edge of the acoustic bulk band. As explained above, strong combination losses make the detection of weak additional features impossible.

The character of such surface phonon gap modes is essentially determined by the difference between the large cation mass $m_c$ and the small anion mass $m_a$. In the opposite case, when $m_a > m_c$, no similar gap modes are expected. Theoretical studies on AlSb(110) and GaSb(110) surfaces revealed that the corresponding phonon branches are located in the acoustic bulk continuum and even mix with bulk states.[3] For AlSb(110), the experiment gives a mode very close to the optical band edge in good agreement with the theoretical predictions. The calculated displacement pattern exhibits motions of second- and third-layer cations normal to the surface. For GaSb(110) no surface phonons within the gap were predicted by theory.[3] This is confirmed by the experimental data. Therefore, the present study agrees excellently with the theoretical prediction. Gap modes appear clearly only if $m_a$ is much smaller than $m_c$. If $m_a > m_c$, gap modes—if existing at all—split off from the optical bulk phonon band and are very close to its band edge.

### B. Fuchs-Kliewer phonons

FK phonons are well-characterized surface excitations in the long-wavelength limit.[25] They are accompanied with long-range electromagnetic fields. Hence, a theoretical approach including macroscopic quantities from electrodynamics describes the nature of these vibrations very well.[29,39] The excitation energies $\hbar\omega_{\mathrm{FK}}$ of the FK phonons may be deduced from the frequencies $\omega_{\mathrm{TO}}$ of TO phonons by a modified Lyddane-Sachs-Teller relation,

$$\left(\frac{\omega_{\mathrm{FK}}}{\omega_{\mathrm{TO}}}\right)^2 = \frac{1+\varepsilon_s}{1+\varepsilon_\infty}. \tag{2}$$

The quantities $\varepsilon_s$ and $\varepsilon_\infty$ denote the static and electronic dielectric constants, respectively. This equation is excellently fulfilled for most of the infrared active dielectric materials. Figure 10 demonstrates the almost 1:1 relationship between calculated and measured FK excitation energies for III-V compound semiconductors. The calculated values were deduced from experimental data for $\varepsilon_s$, $\varepsilon_\infty$ and $\omega_{\mathrm{TO}}$ taken from the literature (references in Refs. 28 and 40).

From the microscopic point of view, one may define a force constant

$$F_{\mathrm{FK}} := \mu(\hbar\omega_{\mathrm{FK}})^2, \tag{3}$$

where $\mu$ represents the reduced mass of an anion-cation pair. Such force constants of III-V compound semiconductors were introduced earlier to find mass trends in phonon energies.[2,17,20] They still depend on the lattice constants or the nearest-neighbor distances $d_{\mathrm{nn}}$. This is shown in Fig. 11 for FK phonons. The force constant is plotted against $d_{\mathrm{nn}}$,

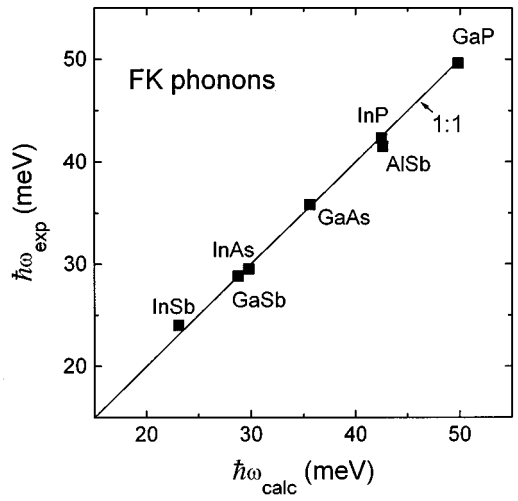


FIG. 10. Excitation energies of Fuchs-Kliewer phonons of III-V semiconductors extracted from HREEL spectra and using Eq. (2).

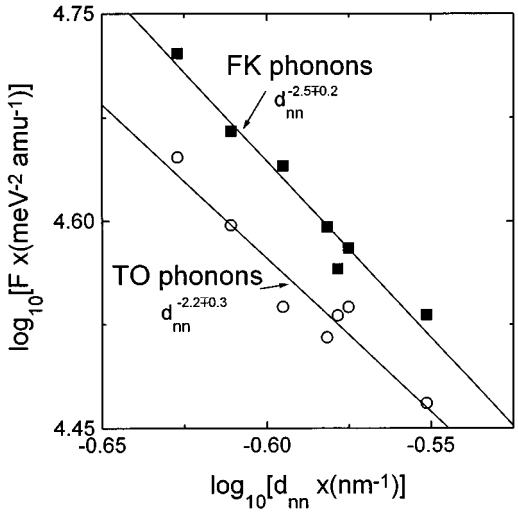


FIG. 11. Force constants, as defined in Eq. (3), of FK surface and TO bulk phonons of III-V semiconductors as a function of the nearest-neighbor distance.

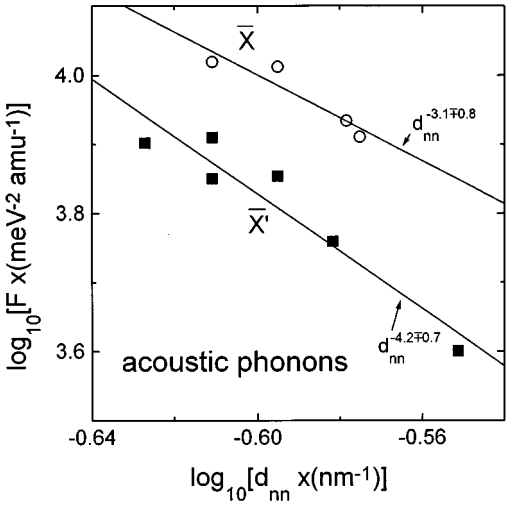


FIG. 12. Force constants, as defined in Eq. (5), of III-V surface acoustic phonons as a function of the nearest-neighbor distance. The excitation energies were taken at $\bar{X}$ and $\bar{X}'$.

both on logarithmic scales to base 10. The solid line is a linear least-squares fit to the data points. To good approximation, one finds

$$F_{\mathrm{FK}} \propto d_{\mathrm{nn}}^{-2.5} \Leftrightarrow \omega_{\mathrm{FK}}^2 \propto \frac{1}{\mu d_{\mathrm{nn}}^{2.5}}. \tag{4}$$

The error in the exponent is about $\pm 0.2$. TO bulk phonon energies show a similar relation. They scale with $d_{\mathrm{nn}}^{-2.2\pm0.3}$ as shown in Fig. 11 as well. Obviously, the scaling rule is better fulfilled for FK than for TO phonons.

### C. Acoustic surface phonons

From the mass dependence of sound velocities in simple linear chain models Tütüncü and Srivastava suggested that the energies of acoustic surface phonons at the main symmetry points scale with the sum of anion and cation masses.[17] They checked the proposal with theoretical data obtained by using the bond-charge concept. A respective force constant may be defined as

$$F_A := (m_a + m_c)(\hbar \omega_A)^2. \tag{5}$$

Again, $F_A$ depends on $d_{\mathrm{nn}}$ as presented in Fig. 12 for the s-BZ points $\bar{X}$ and $\bar{X}'$. Data from HAS experiments[4,5,8] are also included. This method resolves the different phonon branches at $\bar{X}'$. In Fig. 12 only the high-energy modes detected with HAS are considered. The least-squares fits through the points in Fig. 12 give exponents of $-3.1\pm0.8$ and $-4.2\pm0.7$. If one considers the elastic constants in a very simple rigid hybrid model using empirical tight binding parameters[41] one would expect a $d_{\mathrm{nn}}^{-4}$ dependence. The values found for the acoustic modes are close to that prediction.

## V. SUMMARY

This study presents surface phonon dispersions obtained with HREELS at AlSb(110), InAs(110), GaP(110), and GaSb(110) surfaces. The acoustic surface waves are well observed in all materials. Besides, several almost flat optical phonon branches are found. At AlSb(110), at least four optical surface phonons are detected. One of them is located in the fundamental gap between optical and acoustic bulk phonon bands. It is found very close to the optical band edge. In the case of GaP(110), a couple of modes are clearly observed in the middle and upper half of the band gap. In GaSb(110), only loss structures with energies within the bulk continuum are found. The detection of microscopic phonons in InAs(110) is almost impossible due to excitation of surface plasmons. At the s-BZ boundary and in the second s-BZ some losses could be assigned to surface phonons.

The present experimental results are in excellent agreement with theoretical dispersion curves calculated from first principles. They confirm the picture deduced from theory that pronounced gap modes in III-V(110) surfaces exist only in cases where the cation mass is larger than the anion mass. In the opposite case the gap may be even free of surface-localized states, as in case of GaSb(110).

Together with results reported earlier, scaling rules and chemical trends are presented for the excitation energies of FK and acoustic surface phonons demonstrating that the dynamics of the III-V compounds are very similar. The energies may be well approximated by the masses of anions and cations, the nearest-neighbor distances and a constant independent of the material.

The effect of the mass difference between anion and cation on the existence of gap modes is also expected for zinc-blende II-VI semiconductor surfaces. Also cleaved surfaces of wurtzite structure semiconductors may show gap modes that are influenced by the anion-cation mass difference. However, to verify this expectation experimental and theoretical work on these materials is certainly needed.

## ACKNOWLEDGMENTS

The AlSb crystals used in this study were kindly provided by Dr. H. Bender and Professor Dr. E. Schönherr of the Max-Planck-Institut of Solid State Research in Stuttgart. This is gratefully acknowledged. The author thanks Professor Dr. W. Mönch for the critical reading of the manuscript.

*FAX: ++49-203-379-2709. Electronic address: nienhaus@uni-duisburg.de

[1] *Surface Phonons*, edited by W. Kress and F. W. de Wette, Springer Series in Surface Science Vol. 21 (Springer, Berlin, 1991).

[2] H. Nienhaus, in *Festkörperprobleme–Advances of Solid State Physics*, edited by R. Helbig (Vieweg, Wiesbaden/Braunschweig, 1997), Vol. 36, p. 159.

[3] J. Fritsch, C. Eckl, P. Pavone, and U. Schröder, in *Festkörperprobleme–Advances of Solid State Physics* (Ref. 2).

[4] R. B. Doak and D. B. Nguyen, J. Electron Spectrosc. Relat. Phenom. **44**, 205 (1987).

[5] U. Harten and J. P. Toennies, Europhys. Lett. **4**, 833 (1987).

[6] H. Nienhaus and W. Mönch, Phys. Rev. B **50**, 11 750 (1994).

[7] H. Nienhaus and W. Mönch, Surf. Sci. **328**, L561 (1995).

[8] M. Buongiorno Nardelli, D. Cvetko, V. De Renzi, L. Floreano, A. Morgante, M. Peloi, and F. Tommasini, Phys. Rev. B **52**, 16 720 (1995).

[9] P. K. Das and R. E. Allen, in *Proceedings of the 20th International Conference on the Physics of Semiconductors, Thessaloniki, Greece, 1990*, edited by E. M. Anastassakis and J. D. Joannopoulos (World Scientific, Singapore, 1990), p. 1473.

[10] Y. R. Wang and C. B. Duke, Surf. Sci. **205**, L755 (1988).

[11] W. Kelin and L. Zijing, Phys. Rev. B **41**, 5312 (1990).

[12] T. J. Godin, J. P. LaFemina, and C. B. Duke, J. Vac. Sci. Technol. B **9**, 2282 (1991).

[13] G. K. Schenter and J. P. LaFemina, J. Vac. Sci. Technol. A **10**, 2429 (1992).

[14] P. Santini, L. Miglio, G. Benedek, U. Harten, P. Ruggerone, and J. P. Toennies, Phys. Rev. B **42**, 11 942 (1990).

[15] P. Santini, L. Miglio, G. Benedek, and P. Ruggerone, Surf. Sci. **241**, 346 (1991).

[16] H. M. Tütüncü and G. P. Srivastava, J. Phys. Condens. Matter **8**, 1345 (1996).

[17] H. M. Tütüncü and G. P. Srivastava, J. Phys. Chem. Solids **58**, 685 (1997).

[18] J. Fritsch, P. Pavone, and U. Schröder, Phys. Rev. Lett. **71**, 4194 (1993).

[19] R. Di Felice, A. I. Shkrebtii, F. Finocchi, C. M. Bertoni, and G. Onida, J. Electron Spectrosc. Relat. Phenom. **64/65**, 697 (1993).

[20] W. G. Schmidt, F. Bechstedt, and G. P. Srivastava, Phys. Rev. B **52**, 2001 (1995); Surf. Sci. **352-354**, 83 (1996).

[21] U. Schröder, J. Fritsch, and P. Pavone, Physica B **219-220**, 434 (1996).

[22] J. Fritsch, P. Pavone, and U. Schröder, Phys. Rev. B **52**, 11 326 (1995).

[23] H. M. Tütüncü and G. P. Srivastava, Phys. Rev. B **53**, 15 675 (1996).

[24] Ch. Eckl, P. Pavone, J. Fritsch, and U. Schröder, in *The Physics of Semiconductors, Proceedings of the 23rd International Conference, Berlin, 1996*, edited by M. Scheffler and R. Zimmermann (World Scientific, Singapore, 1996), p. 229.

[25] R. Fuchs and K. L. Kliewer, Phys. Rev. **140**, A2076 (1965); **144**, 495 (1966); in *Advances in Chemical Physics*, edited by I. Prigogine and S. A. Rice (Wiley, New York, 1974), Vol. 27, p. 355.

[26] H. Ibach, M. Balden, D. Bruchmann, and S. Lehwald, Surf. Sci. **269/270**, 94 (1992).

[27] D. L. Mills, Surf. Sci. **158**, 411 (1988).

[28] W. Mönch, *Semiconductor Surfaces and Interfaces*, 2nd ed. (Springer, Berlin, 1995).

[29] H. Ibach and D. L. Mills, *Electron Energy Loss Spectroscopy and Surface Vibrations* (Academic, New York, 1982).

[30] L. H. Dubois and G. P. Schwartz, Phys. Rev. B **26**, 794 (1982).

[31] Y. Chen, D. J. Frankel, J. R. Anderson, and G. J. Lapeyre, J. Vac. Sci. Technol. A **6**, 752 (1988).

[32] Y. Chen, J. C. Hermanson, and G. J. Lapeyre, Phys. Rev. B **39**, 12 682 (1989).

[33] P. A. Thiry, J. L. Longueville, J. J. Pireaux, R. Caudano, H. Munekata, and M. Liehr, J. Vac. Sci. Technol. A **5**, 603 (1987).

[34] C. Eckl, P. Pavone, J. Fritsch, and U. Schröder (private communication).

[35] D. Strauch, B. Dorner, and K. Karch, in *Proceedings of the 3rd International Conference on Phonon Physics, Heidelberg, 1989*, edited by S. Hunklinger, W. Ludwig, and G. Weiss (World Scientific, Singapore, 1990), p. 82.

[36] R. K. Ram and S. S. Kushwara, J. Phys. Soc. Jpn. **54**, 617 (1985).

[37] D. L. Rice, J. M. Rowe, and R. M. Nicklow, Phys. Rev. B **3**, 1268 (1971).

[38] A. Ritz and H. Lüth, Phys. Rev. Lett. **52**, 1242 (1984).

[39] H. Lüth, *Surfaces and Interfaces of Solids*, 2nd ed. (Springer, Berlin, 1993).

[40] *Semiconductors—Group IV Elements and III–V Compounds*, edited by O. Madelung (Springer, Berlin, 1991).

[41] W. A. Harrison, *Electronic Structure and the Properties of Solids* (Freeman, San Francisco, 1980).